Research Article | Vol. 29, No. 10 / 10 May 2021 / Optics Express 15452
Optics EXPRESS

Interference fading suppression in φ-OTDR using space-division multiplexed probes

ZHIYONG ZHAO,[1,4] HUAN WU,[2,4] JUNHUI HU,[2,3] KUN ZHU,[2,*] YUNLI DANG,[1] YAXI YAN,[2] MING TANG,[1] AND CHAO LU[2]

[1] *Wuhan National Laboratory for Optoelectronics (WNLO), School of Optics and Electronic Information, Huazhong University of Science and Technology, Wuhan 430074, China*
[2] *Photonics Research Centre, Department of Electronic and Information Engineering, The Hong Kong Polytechnic University, Hong Kong, China*
[3] *Guangxi Key Laboratory of Nuclear Physics and Technology, College of Physics Science and Technology, Guangxi Normal University, Guilin 541004, China*
[4] *These authors contributed equally to this work*
[*] *kenny.kun.zhu@gmail.com*

Abstract: We propose and experimentally demonstrate a novel interference fading suppression method for phase-sensitive optical time domain reflectometry (φ-OTDR) using space-division multiplexed (SDM) pulse probes in a few-mode fiber. The SDM probes consist of multiple different modes, and three spatial modes (LP01, LP11a, and LP11b) are used in this work for the proof of concept. Firstly, the Rayleigh backscattering light of different modes is experimentally characterized, and it turns out that the waveforms of the φ-OTDR traces for distinct modes are all different and independent. Thanks to the spatial difference of the fading positions for distinct modes, multiple probes from spatially multiplexed modes can be used to suppress the interference fading in φ-OTDR. Then, the performances of the φ-OTDR systems using a single probe and multiple probes are evaluated and compared. Specifically, the statistical analysis shows that the fading probabilities over both the fiber length and the time scale are reduced significantly by using multiple SDM probes, which verifies the significant performance improvement on fading suppression. By introducing the concept of SDM to φ-OTDR, the proposed novel interference fading suppression method avoids the complicated frequency or phase modulation, which has the advantages of simplicity, good effectiveness and high reliability.

1. Introduction

Phase-sensitive optical time domain reflectometry (φ-OTDR) has attracted a lot of research interests in the last decade, owing to its outstanding performance of distributed vibration sensing, which has shown great potential in various applications, e.g., intrusion monitoring, railway transportation monitoring, pipeline safety monitoring, seismic monitoring [1–4], etc.

In recent years, to achieve quantitative vibration frequency detection, the optical phase instead of optical amplitude of Rayleigh backscattering signal is usually used in φ-OTDR. This is because the phase change is linear to the external vibration, which ensures the high fidelity of the vibration measurement. The optical phase can be obtained using coherent detection method. However, the coherent detection based φ-OTDR sensors suffer from signal fading issues, including polarization fading and interference fading. The polarization fading results from the polarization mismatch between the Rayleigh backscattered light and the local oscillator. This problem can be solved using polarization diversity detection [5,6]. On the other hand, the interference fading originates from the coherent Rayleigh interference. Since the refractive index distribution of fiber core is not uniform but random, the detected φ-OTDR intensity trace may have some very weak points due to the destructive interference. The demodulated phases at those backscattering points with

#422608 https://doi.org/10.1364/OE.422608
Journal © 2021 Received 12 Feb 2021; revised 17 Apr 2021; accepted 27 Apr 2021; published 5 May 2021

Optics EXPRESS

very low signal-to-noise ratio (SNR) may have severe errors as they are companied with large noise, which eventually leads to frequent false alarms.

Several solutions have been proposed to suppress the interference fading. The concept of frequency-division multiplexing (FDM) was firstly introduced to the φ-OTDR for providing multi-frequency probes to solve the fading problem [7–12]. It is found that the fading positions of φ-OTDR traces are frequency-dependent, thus multiple Rayleigh backscattering traces obtained from optical pulses with different frequencies help to mitigate the misjudgment [7]. Since then, various FDM-based methods using different frequency modulation schemes have been reported, e.g., using multiple acousto-optic modulators (AOMs) or an additional electro-optic modulator (EOM) to generate the optical pulses with different frequencies [8–11]. Inner-pulse frequency-division scheme has also been proposed, where multiple equivalent probes were obtained from a linear-frequency-modulated pulse, and the phases were aggregated with the rotated-vector-sum method to effectively remove the fading noise [13,14]. Based on the acquisition of multiple FDM probes, other processing methods have been developed, such as the spectrum extraction and remix method, as well as the spectrum extraction and phase-shift transform method [15–17]. Besides, using probes with different phase shifts turns out to be another effective solution to suppress the interference fading, since it is proved that the fading positions of the φ-OTDR traces vary if optical pulses with different phase shifts are injected [18]. In summary, all these FDM-based fading-suppression schemes require additional modulation and demodulation procedures, which indeed solve the interference fading problem efficiently, but also bring extra complication and difficulty to the φ-OTDR sensors.

Recently, multimode fiber has been reported to be used in φ-OTDR systems [19–22]. A typical multimode fiber can usually support hundreds of spatial modes, which cannot be easily and separately demodulated with standard photodetectors in conventional φ-OTDR systems. In addition, the severe mode coupling issue in multimode fiber will further degrade the performance of the φ-OTDR sensors. Nevertheless, special techniques have been adopted to collect the different backscattering signals from several spatial modes out of a multimode fiber for fading suppression, such as using a high-speed camera [19,20] or using a home-made conjunction fiber splitter [21]. Though these multimode fiber-based φ-OTDR sensors are immune to the fading, the usage of multimode fiber might degrade the sensors' performance. Moreover, those specially designed optical structures or devices would make the sensor complicated and incompatible with the standard φ-OTDR. It is also realized that the characteristics of Rayleigh backscattering signal of a specific mode in multimode fiber instead of multiple mixed modes has not been investigated yet.

In this work, we propose and experimentally demonstrate a novel scheme for the interference fading suppression in φ-OTDR under the concept of space-division multiplexing (SDM). To the best of our knowledge, this is the first time that a few-mode fiber (FMF) is introduced to the φ-OTDR to generate multiple SDM probes for fading suppression. Due to the low mode coupling property of the FMF, the characteristics of Rayleigh backscattering signal (RBS) for different spatial modes is experimentally investigated using a three-mode fiber. We first prove that the three modes exhibit unique waveforms with weak correlation, thus can be aggregated for suppressing the interference fading. With the usage of the FMF and standard commercial components, we build a fading-free φ-OTDR system with 4.82 km few-mode sensing fiber and 5 m spatial resolution. By aggregating different spatial modes, the performance of φ-OTDR with single and multiple probes is qualitatively and quantitatively analyzed. Based on the detailed statistical analysis, it turns out that the fading probability can be significantly reduced by aggregating and jointly analyzing the SDM probes. Our work provides a new approach to suppress the interference fading in φ-OTDR, which is efficient and easy to realize.

Optics EXPRESS

2. Experimental setup

To investigate the characteristics of Rayleigh backscattering signals of different spatial modes, a three-mode fiber which supports LP01, LP11a and LP11b modes has been used in the experiment. The refractive index profile of the used three-mode fiber is shown in Fig. 1(a), which has a grade-index distribution. The mode profiles of LP01, LP11a and LP11b are presented in Fig. 1(b).

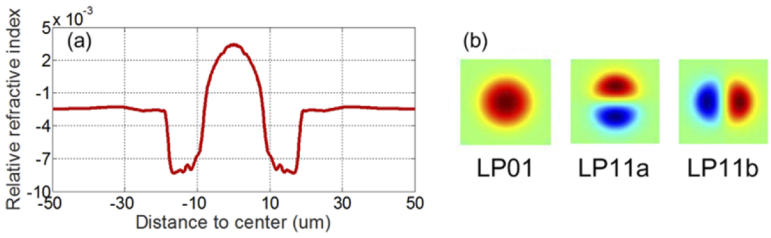

Fig. 1. (a) Refractive index profile of the used three-mode fiber and (b) schematic diagrams of mode profiles of the three modes, respectively.

A heterodyne-based φ-OTDR system with coherent-detection configuration is used in the experiment, whose setup is shown in Fig. 2. A 100 Hz narrow-linewidth coherent laser (NKT Photonics X15) is used as the optical source, whose output is split into two branches through an optical coupler. The upper branch is used to generate the probe pulse through an acousto-optic modulator (AOM, G&H T-M080-0.4C2J-3-F2S) with an 80 MHz frequency shift. The used pulse width is 50 ns, which corresponds to 5 m spatial resolution. The optical pulse is then amplified by an erbium-doped fiber amplifier (EDFA, Amonics AEDFA-18-M-FA), which is followed by a 0.8 nm optical bandpass filter to remove the amplified spontaneous emission (ASE) noise. The boosted pulse is then divided into three branches, which will be used for the interrogations of different spatial modes, i.e., LP01, LP11a and LP11b modes, respectively. The multiplexing/de-multiplexing of the three modes is achieved with the help of a mode-selective photonic lantern with nominal mode-extinction ratio larger than 18 dB, which ensures good mode conversion between the single-mode fibers (SMFs) and the FMF [23–25]. The pulses are launched into the three ports of the photonic lantern after passing through three optical circulators, respectively. The used three-mode fiber in the experiment has a length of 4.82 km. On the other hand, the lower branch is served as the optical local oscillator, which is also divided into three branches. At the receiver side of each mode, the Rayleigh backscattering light will mix with the

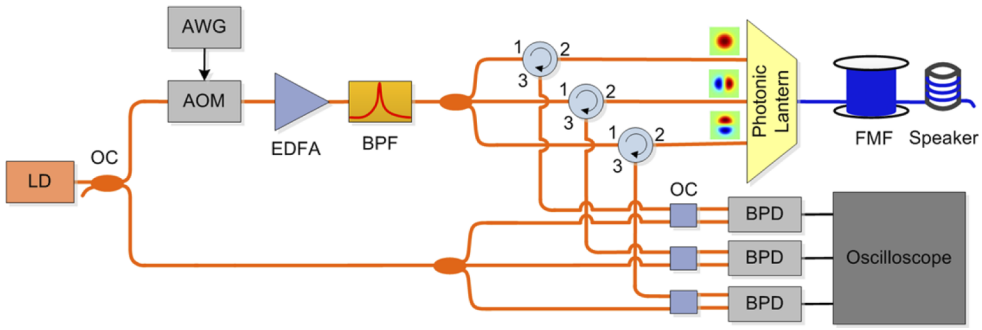

Fig. 2. Experimental setup of the few-mode fiber based φ-OTDR sensing system. LD: laser diode; OC: optical coupler; AOM: acousto-optic modulator; AWG: arbitrary waveform generator; EDFA: erbium-doped fiber amplifier; BPF: band-pass filter; FMF: few-mode fiber; BPD: balanced photo detector.

Optics EXPRESS

local oscillator, and three balanced photodiodes (BPDs, KY-BPRM-BW-I-FA) are used to detect the beating signals, respectively. In the experiment, the vibration is applied through a speaker with 10 m fiber sticked on it at around 4.75 km as mentioned in [26]. The data of all the mode channels are collected simultaneously by an oscilloscope (Keysight MSOS404A). The acquired data are then processed in the digital domain. Eventually, both the optical intensity and phase of Rayleigh backscattering light can be demodulated.

3. Experimental results and discussions

We firstly investigate the characteristics of Rayleigh backscattering signals of different spatial modes. Since the RBS of each mode is detected independently, the RBS intensity and phase information of each mode can be obtained directly using the respective data. Figures 3(a1)–3(a3) show the demodulated optical intensity along the whole fiber length for LP01, LP11a and LP11b modes, respectively. It is observed that many locations have very weak optical intensity, even lower than the noise floor at some positions due to the severe interference fading. Correspondingly, Figs. 3(b1)–3(b3) show the demodulated differential optical phase of the three modes respectively, and each contains 100 differential phase traces. Significant phase fluctuations induced by the interference fading can be observed within the whole fiber length, while only one vibration is applied to the sensing fiber at 4.75 km. Large phase errors will make it impossible to identify the vibrations correctly, and the frequent false alarms will make the φ-OTDR system unusable. In order to compare the characteristics of the RBS from different spatial modes, the demodulated optical intensity and phase of all the three modes are plotted together in Figs. 3(a4) and 3(b4), respectively. The zoom-in view of the traces from 4592 m to 4800 m are presented to show the details of the waveforms. Figure 3(a4) indicates that the waveforms of the RBS traces of diverse spatial modes are different from each other, where the fading points of different modes take place at distinct locations. The correlation coefficients between the modes have been calculated in order to evaluate their correlation. The calculated correlation coefficients are −0.0215 for LP01 and LP11a modes, −0.1473 for LP01 and LP11b modes, and 0.1005 for LP11a and LP11b modes, respectively. The differential optical phase traces of different modes presented in Fig. 3(b4) also show the difference between the distinct modes. Due to the severe phase errors caused by the interference fading, the reliability of the sensing system will be very bad if only one mode is used.

The waveforms in Fig. 3 indicate that the interference fading in φ-OTDR can be addressed by aggregating the multiple SDM probes from different spatial modes. To verify the feasibility, the Rayleigh backscattering signals of the probes from different spatial modes are aggregated using the rotated vector sum method to investigate the characteristics of the synthesized signals [13]. Figures 4(a1) and 4(a2) show the demodulated optical intensity of the aggregated RBSs from two modes, including the combination of the fundamental mode and a high-order mode, i.e., LP01+LP11a, and the combination of two high-order modes, i.e., LP11a + LP11b, respectively. It is observed that the interference-fading-induced intensity fluctuation is reduced. The lowest optical intensity of the LP01+LP11a aggregation is 2.5 dB higher than the noise floor, and that is 1.9 dB for the LP11a + LP11b aggregation. The less SNR improvement may be due to the high correlation between the two degenerate modes LP11a and LP11b. Meanwhile, the demodulated differential optical phase of the aggregated RBSs from two modes is shown in Figs. 4(b1) and 4(b2), correspondingly. Compared with the result of each single probe as shown in Fig. 3, it is seen that the probability of the phase errors due to the interference fading is reduced notably. To further investigate the performance of the φ-OTDR system with the aggregation of multiple probes from different spatial modes, all the three modes are then used. The demodulated optical intensity after aggregation is shown in Fig. 4(a3). The lowest optical intensity is 5 dB higher than the noise floor, which shows a better fading suppression in comparison with the case of the two-probe aggregation. Figure 4(b3) shows the demodulated differential optical phase after aggregation of the three modes. It is seen that the phase errors due to the interference fading are eliminated

Optics EXPRESS

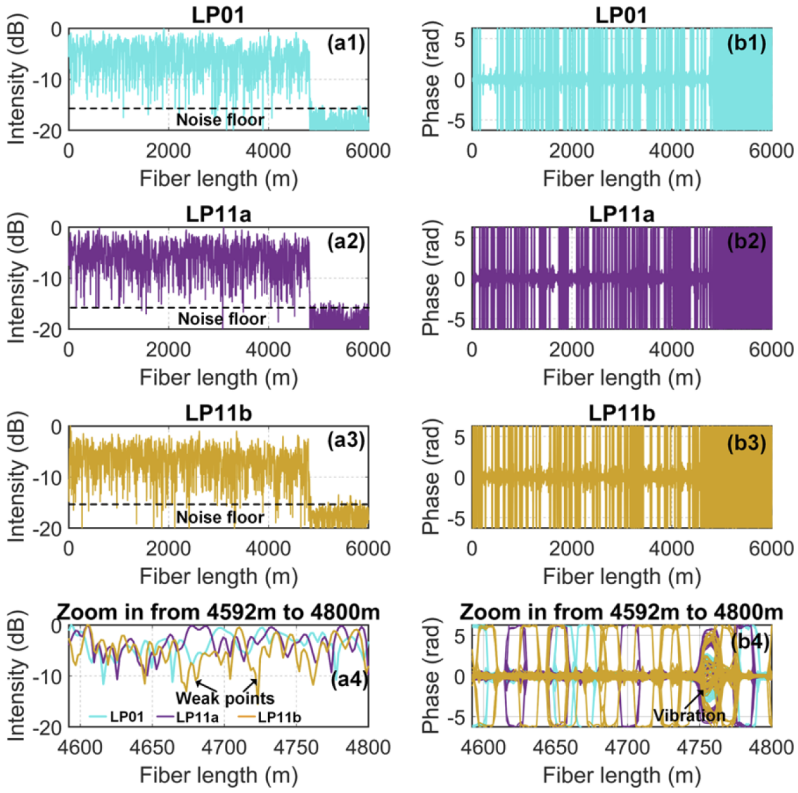

Fig. 3. (a1)–(a3) are the demodulated optical intensity of Rayleigh backscattering signals of the three modes, respectively; (a4) is the zoom-in view of optical intensity traces of the three modes between 4592 m and 4800 m; (b1)–(b3) are the demodulated optical phase of Rayleigh backscattering signals of the three modes, respectively; (b4) is the zoom-in view of optical phase traces of the three modes between 4592 m and 4800 m.

completely, which verifies the excellent feasibility of the fading suppression using multiple SDM probes with several modes. To compare the performance of the aggregation of two modes and three modes, the demodulated intensity and differential phase after different aggregations are plotted in Figs. 4(a4) and 4(b4), respectively, with only the zoom-in view between 4592 m and 4800 m. The result indicates that the intensity fluctuation with the three-mode aggregation is less than that of the two-mode aggregation. Meanwhile, it also shows that aggregating two modes cannot completely eliminate the fading-caused phase errors; however, after aggregating three modes, an φ-OTDR system immune to fading error and false alarm can be achieved. The results demonstrate that the fading issue in φ-OTDR can be addressed by aggregating several probes with different modes, and better suppression performance with more modes can be expected.

To quantitatively compare the characteristics of the single-probe and multi-probe aggregated signals, the fading probabilities over both the fiber length and the time scale are analyzed statistically. Firstly, histograms of the normalized optical intensity of φ-OTDR traces within one period are calculated, as shown in Fig. 5(a1). For the single-probe signals (i.e., LP01, LP11a or LP11b mode), the histograms exhibit typical Rayleigh distribution with peaks located at around 0.2 (−6.99 dB), indicating that many locations tend to occur fading, which matches well with the waveforms in Figs. 3(a1)–3(a3). If two modes are aggregated (e.g., LP01+LP11a or LP11a + LP11b), the histograms are obviously right shifted with peaks centered at 0.32 (−4.95 dB). This indicates that the fading probability will be greatly reduced because the probability of the

Optics EXPRESS

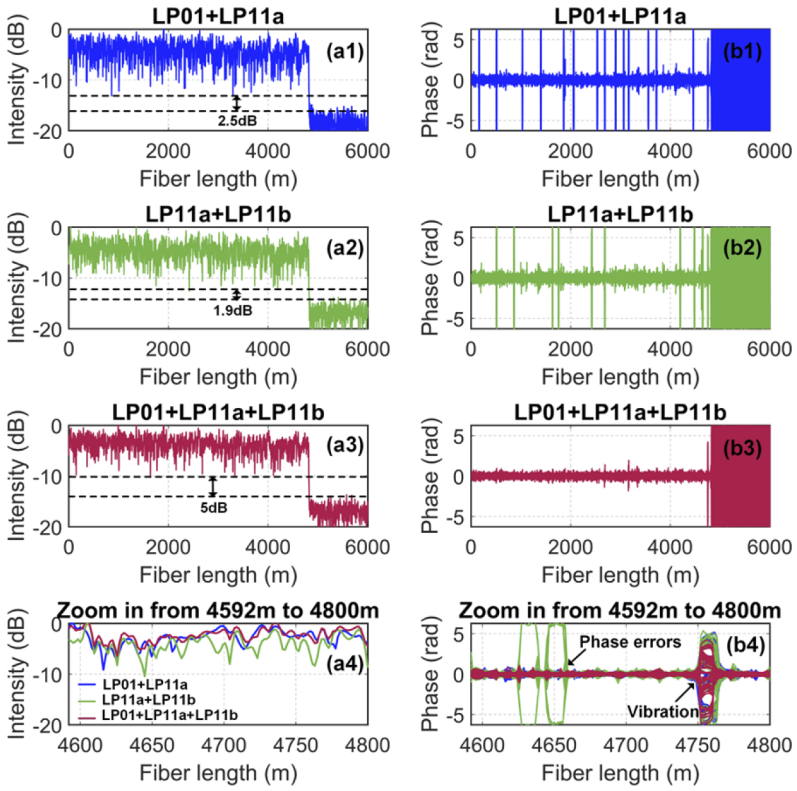

Fig. 4. (a1)–(a3) are the demodulated optical intensity of the aggregated RBSs of LP01+LP11a, LP11a + LP11b, and LP01+LP11a + LP11b modes, respectively; (a4) is the zoom-in view of optical intensity traces between 4592 m and 4800 m; (b1)–(b3) are the demodulated optical phase of the aggregated RBSs of LP01+LP11a, LP11a + LP11b, and LP01+LP11a+ LP11b modes, respectively; (b4) is the zoom-in view of optical phase traces between 4592 m and 4800 m.

low intensity is decreased. It is worth mentioning that the histograms have no big difference between the aggregation of one fundamental mode and one high-order mode (i.e., LP01+LP11a), and the aggregation of two high-order modes (i.e., LP11a + LP11b). In addition, the normalized intensity histogram of the three-mode aggregated signal (i.e., LP01+LP11a + LP11b) is also plotted. The peak center is further right shifted to 0.42 (−3.77 dB), suggesting that the fading probability may be further reduced by aggregating more probes. Cumulative distribution function (CDF) is then calculated to characterize the corresponding histogram, as shown in Fig. 5(b1). The CDF curves are very close if the same number of probes are used, e.g., for single probe (LP01, LP11a, and LP11b mode) or two probes (LP01+LP11a or LP11a + LP11b). However, with the aggregation of more probes, the CDF curve is more right shifted. Considering using 0.1 (−10 dB) as the threshold, the percentages of points below the threshold are 11.72%, 11.18%, and 9.72% for LP01, LP11a, and LP11b, respectively. The percentages are decreased significantly to 0.77% and 0.59% for LP01+LP11a and LP11a + LP11b aggregated signals, respectively. For LP01+LP11a + LP11b, there is no point lower than the threshold, which shows that a fading-free φ-OTDR system is achieved.

Due to the random nature of Rayleigh backscatters, the interference fading will not only occur along the fiber, but also happen with the time. Statistical analysis is also carried out by investigating the fading probability of a random but fixed location on the same sensing fiber. We

Optics EXPRESS

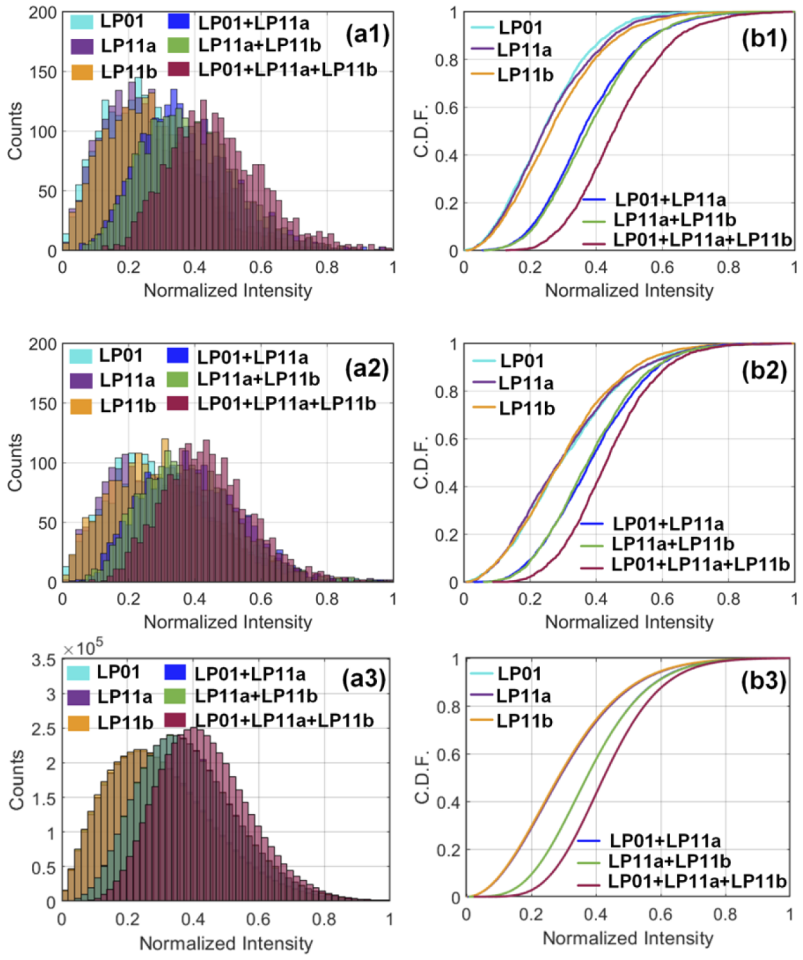

Fig. 5. (a1)–(a3) are the probability distributions of the normalized optical intensity of φ-OTDR for all the sensing points along the fiber length within one period (a1), for a random sensing point over 2000 φ-OTDR traces (a2), and for all the sensing points along the fiber length over 2000 φ-OTDR traces (a3), respectively; (b1)–(b3) are the corresponding cumulative distribution functions to the data in (a1)–(a3), respectively.

acquired 2000 φ-OTDR traces once every 0.8 s with the total acquisition time of 1600 s. The histograms of the normalized intensity over this period at 4 km location are drawn in Fig. 5(a2). The statistical result shows a similar trend as that over the whole fiber length as presented in Fig. 5(a1). Figure 5(b2) shows the corresponding CDF of the normalized intensity at 4 km location over 2000 s. Similar trend can be observed, i.e., by aggregating more probes, the intensity is more likely to be with higher values. Again, if 0.1 (−10 dB) is selected as the threshold, the intensity of LP01, LP11a, and LP11b modes may have 10%, 8.2%, and 8.7% probabilities below the threshold, respectively, while the probabilities for LP01+LP11a and LP11a + LP11b modes are only 0.65%. The probability below the threshold of LP01+LP11a + LP11b mode again exhibits zero. The above statistical analysis, both for all the sensing points along the fiber length and for a specific point over a long period, verifies the effectiveness of the interference fading suppression by aggregating multiple SDM probes from different modes. Figures 5(a3) and 5(b3) show the histograms of the normalized intensity for all the sensing points along the fiber

Optics EXPRESS

length over 2000 φ-OTDR traces (i.e.,1600 s in total), and the corresponding CDF curves. The similar trend can be found as we discussed above. With the statistics of larger number of samples, the probability is found towards unity if the same number of probes are used for aggregation. This further confirms that the aggregation of multiple SDM probes can effectively suppress the interference fading, from a perspective of probability statistics.

Apart from the fading suppression performance, the vibration detection performance of the sensing system is also investigated. The demodulated phase at the vibration location and the extracted vibration frequency spectrum from single probe of LP01, LP11a, and LP11b mode are presented in Fig. 6. No obvious distortion can be observed from the demodulated phase as shown in Figs. 6(a1)–6(a3), which matches well with the truly applied vibration signal with the similarity better than 0.9495. In addition, it shows that the 500 Hz vibration frequency can be extracted correctly at the vibration location. However, significant noise can be observed at some positions in each frequency spectrum [Figs. 6(b1)–6(b3)], which is due to the interference-fading-induced errors. The noise may make it difficult to identify the vibration event correctly but lead to false alarms. It should be mentioned that the weak 500 Hz frequency signal along the fiber in these spectra is generated because the mechanical vibration of the speaker is propagated to the 4.8 km main fiber reel.

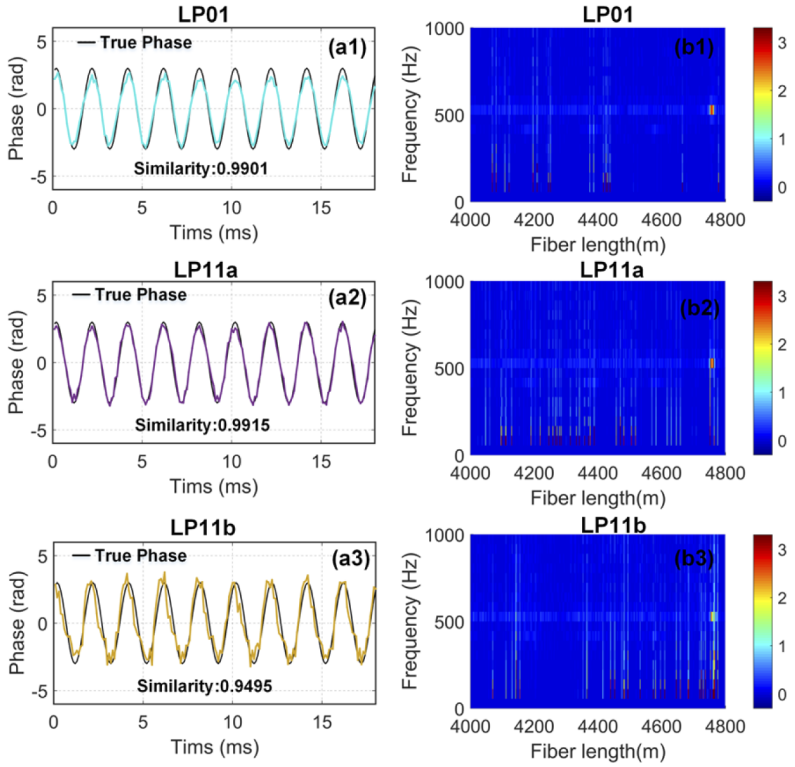

Fig. 6. Vibration detection result using single probe. (a1)–(a3) are the demodulated phases as a function of time at the vibration location; (b1)–(b3) are the extracted vibration frequency spectra along the fiber length.

For comparison, the demodulated phase and the extracted vibration frequency spectra from multi-probe aggregated signal are plotted in Fig. 7. The results indicate that the demodulated phases have good similarity (>0.9816) with the applied vibration signal. Moreover, the interference-fading-induced noise can be effectively reduced in the frequency spectra, particularly

Optics EXPRESS

for the three-probe aggregated case [Fig. 7(b3)], where the noise is totally eliminated. The comparison shows significant performance improvement on the vibration detection against the interference-fading-induced error using multiple SDM probes simultaneously. Finally, it is worth mentioning that mode coupling may take place randomly within the FMF, but as we have shown in the experimental results, it won't degrade the overall performance for fading suppression.

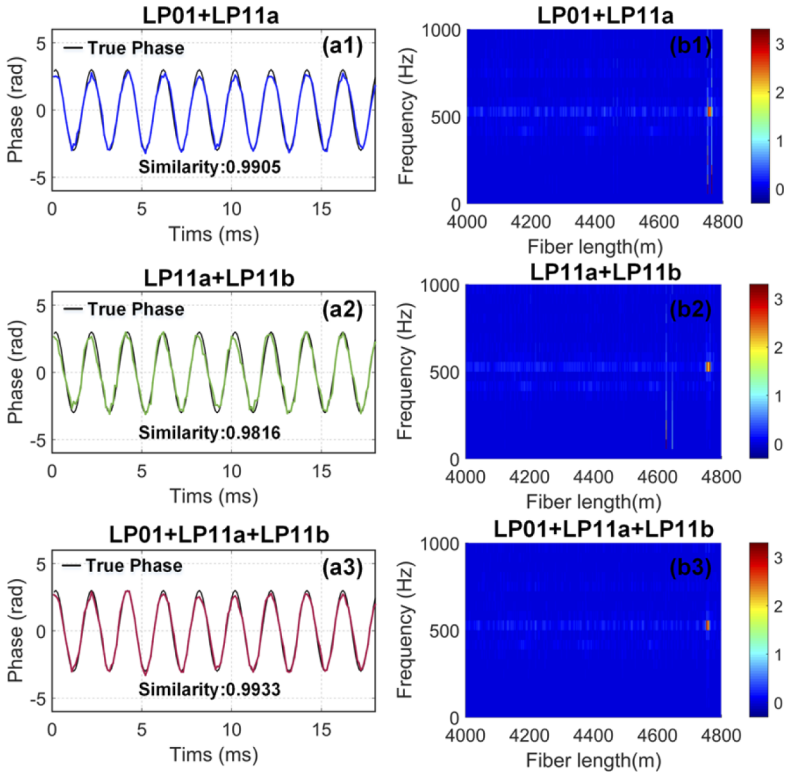

Fig. 7. Vibration detection result using multiple probes simultaneously. (a1)–(a3) are the demodulated phases as a function of time at the vibration location; (b1)–(b3) are the extracted vibration frequency spectra along the fiber length.

4. Conclusion

In conclusion, we propose and demonstrate a novel scheme for interference fading suppression in φ-OTDR under the concept of space-division multiplexing. It is the first time that a few-mode fiber is introduced to the φ-OTDR to solve the fading problem, where the distinct spatial modes are used to generate the SDM probes. It is experimentally observed that the waveforms of the Rayleigh backscattered traces from different spatial modes are distinct from each other, and the possible fading positions also vary for different modes. Based on this, we experimentally prove that the interference fading can be effectively suppressed when three SDM probes with different modes are aggregated and analyzed using the rotated-vector-sum method. In addition, the possibility of fading occurrence is statistically analyzed for different modes and different aggregations. The result shows that the fading probability can be significantly reduced with the aggregation of the three spatial modes, both for all the points along the fiber length and for a specific point during a long period. In summary, we build a fading-free φ-OTDR for accurate detection of the vibration frequency with a 4.85 km few-mode sensing fiber and 5 m spatial resolution. The aggregation of the SDM probes from different modes is easy to achieve with the

Optics EXPRESS

standard components (the photonic lantern and the commercial photodetectors), which provides a simple and effective approach to suppress the interference fading in φ-OTDR.

Funding. National Key Research and Development Program of China (2018YFB1801002); Research Grants Council, University Grants Committee (PolyU 152168/17E); Hong Kong Polytechnic University (PolyU H-ZG7E, YW3G, ZVGB); Guangxi Key Research and Development Program (AB18221033); Guangxi One Thousand Young and Middle-aged College and University Backbone Teachers Cultivation Program (20181227).

Disclosures. The authors declare no conflicts of interest.

References

1. J. C. Juarez, E. W. Maier, K. N. Choi, and H. F. Taylor, "Distributed fiber-optic intrusion sensor system," J. Lightwave Technol. **23**(6), 2081–2087 (2005).
2. F. Peng, N. Duan, Y. J. Rao, and J. Li, "Real-time position and speed monitoring of trains using phase-sensitive OTDR," IEEE Photonics Technol. Lett. **26**(20), 2055–2057 (2014).
3. J. Tejedor, H. F. Martins, D. Piote, J. Macias-Guarasa, J. Pastor-Graells, S. Martin-Lopez, P. C. Guillén, F. De Smet, W. Postvoll, and M. González-Herráez, "Toward prevention of pipeline integrity threats using a smart fiber-optic surveillance system," J. Lightwave Technol. **34**(19), 4445–4453 (2016).
4. P. Jousset, T. Reinsch, T. Ryberg, H. Blanck, A. Clarke, R. Aghayev, G. P. Hersir, J. Henninges, M. Weber, and C. M. Krawczyk, "Dynamic strain determination using fibre-optic cables allows imaging of seismological and structural features," Nat. Commun. **9**(1), 2509 (2018).
5. M. Ren, P. Lu, L. Chen, and X. Bao, "Theoretical and experimental analysis of phi-otdr based on polarization diversity detection," IEEE Photonics Technol. Lett. **28**(6), 697–700 (2016).
6. G. Yang, X. Fan, B. Wang, Q. Liu, and Z. He, "Polarization fading elimination in phase-extracted OTDR for distributed fiber-optic vibration sensing," in *OptoElectronics and Communications Conference (OECC) held jointly with 2016 International Conference on Photonics in Switching (PS)*, 2016 21st, (IEEE, 2016), 1–3.
7. J. Zhou, Z. Pan, Q. Ye, H. Cai, R. Qu, and Z. Fang, "Characteristics and explanations of interference fading of a ϕ-OTDR with a multi-frequency source," J. Lightwave Technol. **31**(17), 2947–2954 (2013).
8. M. Zabihi, Y. Chen, T. Zhou, J. Liu, Y. Shan, Z. Meng, F. Wang, Y. Zhang, X. Zhang, and M. Chen, "Continuous fading suppression method for Φ-OTDR systems using optimum tracking over multiple probe frequencies," J. Lightwave Technol. **37**(14), 3602–3610 (2019).
9. S. Lin, Z. Wang, J. Xiong, Y. Fu, J. Jiang, Y. Wu, Y. Chen, C. Lu, and Y. Rao, "Rayleigh fading suppression in one-dimensional optical scatters," IEEE Access **7**, 2169–2178 (2019).
10. B. Redding, M. J. Murray, A. Davis, and C. Kirkendall, "Quantitative amplitude measuring φ-OTDR using multiple uncorrelated Rayleigh backscattering realizations," Opt. Express **27**(24), 34952–34960 (2019).
11. A. H. Hartog, L. B. Liokumovich, N. A. Ushakov, O. I. Kotov, T. Dean, T. Cuny, A. Constantinou, and F. V. Englich, "The use of multi-frequency acquisition to significantly improve the quality of fibre-optic-distributed vibration sensing," Geophys. Prospect. **66**(S1), 192–202 (2018).
12. C. Cao, F. Wang, Y. Pan, X. Zhang, X. Chen, Q. Chen, and J. Lu, "Suppression of signal fading with multi-wavelength laser in polarization OTDR," IEEE Photonics Technol. Lett. **29**(21), 1824–1827 (2017).
13. D. Chen, Q. Liu, and Z. He, "Phase-detection distributed fiber-optic vibration sensor without fading-noise based on time-gated digital OFDR," Opt. Express **25**(7), 8315–8325 (2017).
14. D. Chen, Q. Liu, and Z. He, "High-fidelity distributed fiber-optic acoustic sensor with fading noise suppressed and sub-meter spatial resolution," Opt. Express **26**(13), 16138–16146 (2018).
15. Y. Wu, Z. Wang, J. Xiong, J. Jiang, S. Lin, and Y. Chen, "Interference fading elimination with single rectangular pulse in Φ-OTDR," J. Lightwave Technol. **37**(13), 3381–3387 (2019).
16. Y. Wu, Z. Wang, J. Xiong, J. Jiang, and Y. Rao, "Bipolar-coding Φ-OTDR with interference fading elimination and frequency drift compensation," J. Lightwave Technol. **38**(21), 6121–6128 (2020).
17. H. He, L. Yan, H. Qian, Y. Zhou, X. Zhang, B. Luo, W. Pan, X. Fan, and Z. He, "Suppression of the interference fading in phase-sensitive OTDR with phase-shift transform," J. Lightwave Technol. **39**(1), 295–302 (2021).
18. X. Wang, B. Lu, Z. Wang, H. Zheng, J. Liang, L. Li, Q. Ye, and H. Cai, "Interference-fading-free Φ-OTDR based on differential phase shift pulsing technology," IEEE Photonics Technol. Lett. **31**(1), 39–42 (2019).
19. M. J. Murray, A. Davis, and B. Redding, "Multimode fiber ϕ-OTDR with holographic demodulation," Opt. Express **26**(18), 23019–23030 (2018).
20. M. J. Murray and B. Redding, "Distributed multimode fiber ϕ-OTDR sensor using a high-speed camera," OSA Continuum **4**(2), 579–588 (2021).
21. A. E. Alekseev, V. S. Vdovenko, B. G. Gorshkov, V. T. Potapov, and D. E. Simikin, "Fading reduction in a phase optical time-domain reflectometer with multimode sensitive fiber," Laser Phys. **26**(9), 095101 (2016).
22. K. Markiewicz, J. Kaczorowski, Z. Yang, L. Szostkiewicz, A. Dominguez-Lopez, K. Wilczynski, M. Napierala, T. Nasilowski, and L. Thévenaz, "Frequency scanned phase sensitive optical time-domain reflectrometry interrogation in multimode optical fibers," APL Photonics **5**(3), 031302 (2020).
23. T. A. Birks, I. Gris-Sánchez, S. Yerolatsitis, S. G. Leon-Saval, and R. R. Thomson, "The photonic lantern," Adv. Opt. Photonics **7**(2), 107–167 (2015).

Optics EXPRESS

24. S. Yerolatsitis, I. Gris-Sánchez, and T. A. Birks, "Adiabatically-tapered fiber mode multiplexers," Opt. Express **22**(1), 608–617 (2014).
25. S. Leon-Saval, N. Fontaine, J. Salazar-Gil, B. Ercan, R. Ryf, and J. Bland-Hawthorn, "Mode-selective photonic lanterns for space-division multiplexing," Opt. Express **22**(1), 1036–1044 (2014).
26. H. Wu, B. Zhou, K. Zhu, C. Shang, H. Tam, and C. Lu, "Pattern recognition in distributed fiber-optic acoustic sensor using an intensity and phase stacked convolutional neural network with data augmentation," Opt. Express **29**(3), 3269–3283 (2021).